REPORT DOCUMENTATION PAGE

Form Approved
OMB No. 0704-0188

Public reporting burden for this collection of information is estimated to average 1 hour per response, including the time for reviewing instructions, searching existing data sources, gathering and maintaining the data needed, and completing and reviewing this collection of information. Send comments regarding this burden estimate or any other aspect of this collection of information, including suggestions for reducing this burden to Department of Defense, Washington Headquarters Services, Directorate for Information Operations and Reports (0704-0188), 1215 Jefferson Davis Highway, Suite 1204, Arlington, VA 22202-4302. Respondents should be aware that notwithstanding any other provision of law, no person shall be subject to any penalty for failing to comply with a collection of information if it does not display a currently valid OMB control number. **PLEASE DO NOT RETURN YOUR FORM TO THE ABOVE ADDRESS.**

1. REPORT DATE *(DD-MM-YYYY)*	2. REPORT TYPE	3. DATES COVERED *(From - To)*
26-01-2007	Conference Paper PREPRINT	2003 - 2006

4. TITLE AND SUBTITLE
Wavefront Aberration Correction Using Zernike Polynomial Parameterizations of Optical Phased Arrays (PREPRINT)

5a. CONTRACT NUMBER

5b. GRANT NUMBER

5c. PROGRAM ELEMENT NUMBER
63401F

6. AUTHOR(S)
Jeffrey A. Butterworth*, Charles Hindman, Seth Lacy

5d. PROJECT NUMBER
4846

5e. TASK NUMBER
03

5f. WORK UNIT NUMBER

7. PERFORMING ORGANIZATION NAME(S) AND ADDRESS(ES)

Air Force Research Laboratory
Space Vehicles Directorate
3550 Aberdeen Ave SE
Kirtland AFB, NM 87117-5776

University of Colorado*
School of Electrical Engineering
Boulder, CO 80309

8. PERFORMING ORGANIZATION REPORT NUMBER
AFRL-VS-PS-TP-2007-1022

9. SPONSORING / MONITORING AGENCY NAME(S) AND ADDRESS(ES)

10. SPONSOR/MONITOR'S ACRONYM(S)
AFRL/VSSE

11. SPONSOR/MONITOR'S REPORT NUMBER(S)

12. DISTRIBUTION / AVAILABILITY STATEMENT
Approved for public release; distribution is unlimited. (Clearance #VS07-0032)

13. SUPPLEMENTARY NOTES
Accepted for publication in the Proceedings of the AIAA Guidance, 20-23 Aug 07, Myrtle Beach, SC

14. ABSTRACT
High performance laser communication systems require adaptive optics based wavefront correction systems to correct aberrations that result from imperfections in optical hardware and atmospheric conditions. Traditionally, deformable membrane mirrors are used for wavefront correction. These mirrors are bulky and require excessive amounts of power, both of which can be detrimental to a space application. Liquid crystal based optical phased arrays (OPAs) offer an attractive alternative to these traditional devices. This paper presents a method of correcting wavefront aberrations with an OPA device by utilizing phase reconstruction of point-source images and Zernike polynomial parameterizations of the OPA. Limitations of common OPA architectures that reduce the effectiveness of the proposed wavefront correction method will be discussed. A simulation will demonstrate the effectiveness of the proposed technique.

15. SUBJECT TERMS
Laser Communication; Aberrations; Wavefront Correction; OPAs; Optical Phased Arrays

16. SECURITY CLASSIFICATION OF:			17. LIMITATION OF ABSTRACT	18. NUMBER OF PAGES	19a. NAME OF RESPONSIBLE PERSON
a. REPORT	b. ABSTRACT	c. THIS PAGE			Charles Hindman
Unclassified	Unclassified	Unclassified	Unlimited	7	19b. TELEPHONE NUMBER *(include area code)* 505-853-4746

Wavefront Aberration Correction Using Zernike Polynomial Parameterizations of Optical Phased Arrays

Jeffrey A. Butterworth, Charles Hindman, and Seth Lacy

***Abstract*— High performance laser communication systems require adaptive optics based wavefront correction systems to correct aberrations that result from imperfections in optical hardware and atmospheric conditions. Traditionally, deformable membrane mirrors are used for wavefront correction. These mirrors are bulky and require excessive amounts of power, both of which can be detrimental to a space application. Liquid crystal based optical phased arrays (OPAs) offer an attractive alternative to these traditional devices. This paper presents a method of correcting wavefront aberrations with an OPA device by utilizing phase reconstruction of point-source images and Zernike polynomial parameterizations of the OPA. Limitations of common OPA architectures that reduce the effectiveness of the proposed wavefront correction method will be discussed. A simulation will demonstrate the effectiveness of the proposed technique.**

I. Introduction

Ultimately, the effectiveness of a laser communication system reduces to optical power. Aberrations disturbing the wavefront of a laser communications link lead to reduced power which directly increases the communication bit error rate. Correction of these wavefront aberrations is essential to efficient communication with optics. This paper presents a method of correcting wavefront aberrations with an optical phased array (OPA) device by utilizing phase reconstruction of point-source images and Zernike polynomial parameterizations of the OPA. Section II introduces the OPA device and describes its limitations that reduce its effectiveness. Section III discusses Zernike Polynomials and their common use in optics. Section IV presents a common phase reconstruction technique and establishes the initial Zernike parametrization of the OPA. Section V discusses a method for representing Zernike polynomials with the OPA. Last, Section VI summarizes simulation methods and results. Conclusions and plans for future work are discussed in Section VII.

Work supported in part by AFOSR Laboratory Initiative 00VS17COR

J. Butterworth is a student of Electrical Engineering at the University of Colorado at Boulder, Boulder, CO 80309, USA butterwo@colorado.edu

C. Hindman is an Aerospace Research Engineer with the Air Force Research Laboratory, Kirtland AFB, NM 87117, USA charles.hindman@kirtland.af.mil

S. Lacy is an Aerospace Research Engineer with the Air Force Research Laboratory, Kirtland AFB, NM 87117, USA seth.lacy@kirtland.af.mil

II. Background on & Limitations of Optical Phased Arrays

A. OPA Background

Optical phased arrays (OPAs), also known as spatial light modulators, are non-mechanical beam steering and correction devices that utilize liquid crystal technology to alter the phase of a collimated beam of light as desired. The crystals in the OPA can be rotated by applying a voltage across the strips of crystals in the device, as shown in Fig. 1. The amount of rotation of the crystal dictates the change in phase that will be applied to the beam being sent through the OPA. To achieve 2-D steering, the OPA can be fully pixelated (like a CCD device); however, due to difficulty in addressing and controlling the very large number of pixels that a 2-D device would entail, 2-D steering is often achieved by using two 1-D OPAs. Since one OPA can only alter the phase of light down the columns of the device, the two OPAs are mounted orthogonally to achieve complete beam steering and wavefront correction.

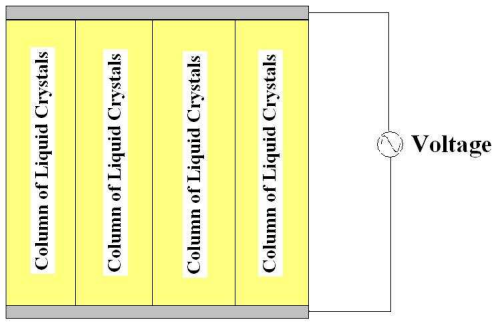

Fig. 1. A view of a simplified OPA with only four strips of liquid crystals. Actual OPA's will have strips on the order of thousands.

This ability to alter the phase of a wavefront provides an alternative to traditional methods that accomplish the same task such as deformable mirrors and steering mirrors. Although often effective, these devices require excessive amounts of power and are heavy, both of which can be detrimental to a space application. OPAs have not yet surpassed the performance levels of the traditional beam steering and correction devices due to various limitations in the technology (that will be discussed later), but their advantages and potential are evident [1].

B. OPA Limitation: Dependent Pixel Relationship

The device of interest is a XY 1x4096 by Boulder Nonlinear Systems [2]. As mentioned in the paragraph above, two orthogonally mounted OPAs are used in this device. This restricts the user's ability to write a desired phase profile to each pixel individually. As a result, the phase change written to a pixel is not independent of pixels sharing the same row of one OPA and column of the other. In Fig. 2, one can see how the phase of the "pixel" x_{11} is the sum of the phase resulting from the voltage input u_1 and u_4. This "non-pixelated" nature of the system is the source of a major limitation when attempting to write desired phase profiles to the device and will be evident in the simulation shown in Section VI.

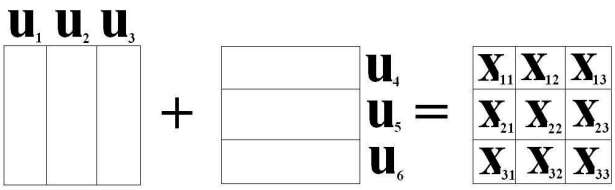

Fig. 2. A simplified view demonstrating the dependence of pixels sharing the same row of one OPA and column of the other. The phase of the "pixel" x_{11} is the sum of the phase resulting from the voltage input u_1 and u_4. Note that the actual OPA will have 4096 u_k inputs on each OPA.

C. OPA Limitation: Parametrization

A device such as the stacked XY beamsteering unit from Boulder Nonlinear Systems consists of two linear OPAs having 4096 control inputs each for a total of 8192 inputs. As a result, a method of parameterizing these inputs is required in order to limit the number of inputs and ease the computational burdens of any electronics working with the OPA. Only the first eleven Zernike polynomials where chosen as the best means for reducing the 8192 inputs to 11 Zernike coefficients. This is because realistic aberrations from physical systems are dominated by the first few Zernikes. In addition, modeling showed that the OPAs cannot reproduce higher order Zernikes due to the dependent pixel relationship of the OPA. Zernike polynomials are a well known method for describing optical aberrations. Their use will be discussed more detail in Section III of this paper.

D. OPA Limitation: Nonlinear Crystal Dynamics

The crystals in an OPA exhibit a nonlinear dynamics. Specifically, when observing same-magnitude step responses, the user will notice a faster rise time to the step towards 2π radians than the same-magnitude step back towards 0 radians. This is because the crystals are forced by the applied voltage when moving towards 2π radians. This is in contrast to moving towards 0 radians where the crystals are relaxing to a natural position of no rotation [3]. In addition, OPA phase profiles are not limited to those described only between 0 and 2π. Profiles that exceed these limits are created by a phase reset in which a modulo 2π property exists. This creates discontinuities in the phase profile represented by the OPA in locations where the the desired phase profile is either less than 0 or greater than 2π. The nonlinearity of the crystal dynamics becomes even more complex in these "fly-back" regions defined by the modulo 2π phase resets. For example, if a crystal is currently oriented at $2\pi - \varepsilon$ (where ε is some arbitrarily small positive value), and if the next phase profile command dictates this crystal should be oriented to $2\pi + \varepsilon$; the crystal will have to "fall" back to ε position at a speed dictated by the slower dynamics. The simulation, shown in Section VI, only considers crystal dynamics between 0 and 2π radians. The complex dynamics associated with phase resets is left to future work.

III. Zernike Polynomials in Optical Systems

Zernike polynomials are commonly used in optics to express wavefront data in polynomial form [4]. Described by a radius ρ and angle θ, they are a complete set of polynomials that are orthogonal over the interior of the unit circle. Zernike polynomials can represent aberrations up to an infinite-order of ρ. However, due to the limitations of the OPA, we will only consider aberrations up to the sixth order. Table I lists the Zernike polynomials used in this study.

TABLE I
Zernike Polynomials

Zernike	Polynomial	Name
z_0	1	Piston
z_1	$\rho\cos(\theta)$	Tilt X
z_2	$\rho\sin(\theta)$	Tilt Y
z_3	$-1+2\rho^2$	Power
z_4	$\rho^2\cos(2\theta)$	Astigmatism X
z_5	$\rho^2\sin(2\theta)$	Astigmatism Y
z_6	$\rho(-2+3\rho^2)\cos(\theta)$	Coma X
z_7	$\rho(-2+3\rho^2)\sin(\theta)$	Coma Y
z_8	$1-6\rho^2+6\rho^4$	Primary Spherical
z_9	$\rho^3\cos(3\theta)$	Trefoil X
z_{10}	$\rho^3\sin(3\theta)$	Trefoil Y
z_{11}	$\rho^2(-3+4\rho^2)\cos(2\theta)$	-
z_{12}	$\rho^2(-3+4\rho^2)\sin(2\theta)$	-
z_{13}	$\rho(3-12\rho^2+10\rho^4)\cos(\theta)$	-
z_{14}	$\rho(3-12\rho^2+10\rho^4)\sin(\theta)$	-
z_{15}	$-1+12\rho^2-30\rho^4+20\rho^6$	-

When describing or simulating an aberration, the sum of a series individual Zernikes is considered. To ensure proper scaling, the Zernike coefficient a_i is introduced. Equation (1) is an example of this for a situation that only considers an aberration up to Zernike z_{15}.

$$Z = a_0 z_0 + a_1 z_1 + a_2 z_2 + ... + a_{14} z_{14} + a_{15} z_{15} \qquad (1)$$

IV. Phase Reconstruction & Initial Zernike Parametrization

A. Method of Phase Reconstruction

The affect of an aberrated phase profile on a series of point sources (often referred to as the object in this document) can be described with an optical transfer function as in (2). The phase profile, $\psi(x, y)$ is the phase as described across a plane (the plane of the OPA, for example). The coordinates x and y describe the location of interest in the plane. Due to this, $\psi(x, y)$ will be a matrix with dimensions corresponding to the size and griding resolution of the OPA. The elements of this matrix will be the value of the phase at the location (x, y) described by the corresponding row and column information of the matrix. The aperture function, $A(u, v)$ is a binary matrix describing the aperture over the plane. A one is inserted in all areas where the aperture is open, whereas a zero is used where the aperture is closed. Most often, the aperture function describes a circle. It is important to note the use of the Hadamard product in (2); standard matrix multiplication is NOT used here. In addition, the exponential in (2) is NOT the matrix exponential. Although $\psi(x, y)$ is a matrix, the exponential in (2) is calculated in an element-wise manner.

$$H(u, v) = A(u, v) \otimes e^{i\psi(x,y)} \quad [1] \tag{2}$$

Note the careful use of (x, y) and (u, v) in (2). As with typical transfer functions, the result of (2) is in the Fourier domain, described here by (u, v). So in order to work with (2), the object of interest must also be in the Fourier domain. Given an object in the spatial domain, $o(x, y)$, the two-dimensional Fourier transform can be used to obtain $O(u, v)$ in the Fourier domain. When using (2) it is not necessary to put the phase profile into the Fourier domain, so it appears as $\psi(x, y)$.

Once a known object can be described in the Fourier domain, the image resulting from sending that object through a phase profile described by the optical transfer function can be described by (3) and (4). Note the use of the Hadamard product in (3).

$$I(u, v) = H(u, v) \otimes O(u, v) \tag{3}$$

$$i(x, y) = \mathcal{F}^{-1}[I(u, v)] \tag{4}$$

With this knowledge, one can rearrange (3) into a form that allows the user to recover the phase profile while only knowing the object, $o(x, y)$ and the image received at the camera, $i(x, y)$. Equation (5) presents this form; it is important to note the use of Hadamard division inside the natural log.

$$\psi(x, y) = -i \ln[I(u, v) \oslash (A(u, v) \otimes O(u, v))] \tag{5}$$

Assuming all the crystals in the OPA are at rest (at zero radians phase profile), a point source can be sent through the OPA. The image received at the camera will be representative of the aberrations in the system. Using (5), one can recover the phase profile associated with the aberration. The negative of this profile associated with the aberration can then be written to the OPA for wavefront correction.

[1]The symbol "$\otimes$" in this document represents the Hadamard product, also know as "dot multiply" in Matlab. The symbol "$\oslash$" in this document represents the Hadamard division, also know as "dot divide" in Matlab.

B. Initial Zernike Parameterization

The result of reconstructing the phase as in Section IV-A presents a recovered phase profile completely described over the plane. Using a least squares fit to this profile, one can parameterize it to the first eleven Zernike polynomials. This allows the profile to be described by only eleven coefficients rather than the entire phase plane worth of data. Again, parametrization is only performed to the first eleven coefficients due to the dependent pixel relationship of the OPA and its inability to decently represent Zernikes beyond this coefficient.

V. OPA Representation of Zernike Polynomials

A. Creating OPA Representations of Zernike Polynomials

Creating a best OPA fit to the eleven-coefficient representation recovered phase profile was done using a least squares method, but in many cases the quality of the fit is severely limited by the orthogonal nature of the pair of OPAs. In the interest of clarity, the fitting method will be described using the simplified OPA example as shown in Fig. 2. Here, there are six u_k inputs and nine $x_{m,n}$ states. To start, the matrix of states needs to be vectorized as in (6) and the inputs must be gathered in vector form as in (7).

$$\vec{x} = [x_{1,1}\ x_{1,2}\ x_{1,3}\ x_{2,1}\ x_{2,2}\ x_{2,3}\ x_{3,1}\ x_{3,2}\ x_{3,3}]^T \tag{6}$$

$$\vec{u} = [u_1\ u_2\ u_3\ u_4\ u_5\ u_6]^T \tag{7}$$

The interest is to create a relationship from input vector to state vector as in (8). The matrix B must be defined as in (9) such that it captures the dependent state relationship. The dimensions of B will always be $(k^2) \times (2k)$ where k is the total number of inputs on one OPA; in this simple example $k = 3$. In addition, B will also always take the form of k blocks of identity matrices down the left half of the matrix with square blocks of unity in advancing columns, down the right half.

$$\vec{x} = B\vec{u} \tag{8}$$

$$B = \left[\begin{array}{ccc|ccc} 1 & 0 & 0 & 1 & 0 & 0 \\ 0 & 1 & 0 & 1 & 0 & 0 \\ 0 & 0 & 1 & 1 & 0 & 0 \\ \hline 1 & 0 & 0 & 0 & 1 & 0 \\ 0 & 1 & 0 & 0 & 1 & 0 \\ 0 & 0 & 1 & 0 & 1 & 0 \\ \hline 1 & 0 & 0 & 0 & 0 & 1 \\ 0 & 1 & 0 & 0 & 0 & 1 \\ 0 & 0 & 1 & 0 & 0 & 1 \end{array}\right] \tag{9}$$

Given a vector representing the desired Zernike phase profile, $\vec{x}_{zern}$, one can define a value function (10) to be minimized when performing least squares. Solving for the $\vec{u}$

that minimizes (10) results in the expression in (11) for the fit optimizing $\vec{u}_{opt}$.

$$V(\vec{x}) = \sum (\vec{x} - \vec{x}_{zern})^2 \tag{10}$$

$$\vec{u}_{opt} = (B^T B)^{-1} B^T \vec{x}_{zern} \tag{11}$$

Due to the structure of B, the matrix $(B^T B)$ is singular making inverting it impossible. As a result, the calculation of $\vec{u}_{opt}$ in (11) is ill-conditioned. The source of this singularity, and a technique to correct the problem becomes clear when looking at the eigenvalues of the matrix $(B^T B)$. In the case of the simplified example with only three inputs per OPA, the eigenvalues of $(B^T B)$ are 0, 3, 3, 3, 3 and 6. The fact that there exists only one zero-valued eigenvalue and that no other eigenvalue are within ± 1 of zero suggests that a small perturbation, δ could be added to the matrix $(B^T B)$ before it is inverted as in (12) where $0 < \delta << 1$.

$$\vec{u}_{opt} = (\delta I + B^T B)^{-1} B^T \vec{x}_{zern} \tag{12}$$

The δ perturbation becomes more robust as the number of inputs per OPA is increased. Specifically, the difference between the zero-value eigenvalue increases linearly by one with each input $\vec{u}_k$ included. For example, when using OPAs with 2048 $\vec{u}_k$ inputs, the difference between the zero-value eigenvalue and the next eigenvalue closest to zero is 2048. At that level, the addition of the δ does not substantially affect the results except to make the calculation possible.

B. The OPA's Limitations in Representing Zernike Polynomials

Due to the orthogonal nature of the pair of OPAs in the Boulder Nonlinear Systems beamsteering device, the representation of a recovered phase profile by the OPA is severely limited. In some cases the OPA can fit a profile with minimal error, in others the result is a poor fit or nonexistent. Fig. 3 presents several examples of OPA Zernike approximations.

VI. Simulation & Results

A. A Model for the Liquid Crystal Dynamics

The nonlinear nature of the liquid crystal dynamics was captured with the use of two linear first order models with an appropriate time constant for each, see (13) and (14). In simulation, an "if statement" is used to select the proper crystal model based on the direction of rotation of the crystal. Based on experimental work by Harris [5], time constants for "falling" and "rising" crystals were modeled respectively as $\tau_{fall} = 12$ and $\tau_{rise} = 4.9$ milliseconds. It is clear that this simplified model will not fully capture all the interesting dynamics of the crystals as it assumes that all crystals located in one input column will all have the same orientation. This is not necessarily true as in reality crystals near the ends of the columns will not rotate as much as those located in the middle of the column [1]. Regardless, this model will be sufficient in helping to validate the proposed wavefront correction technique

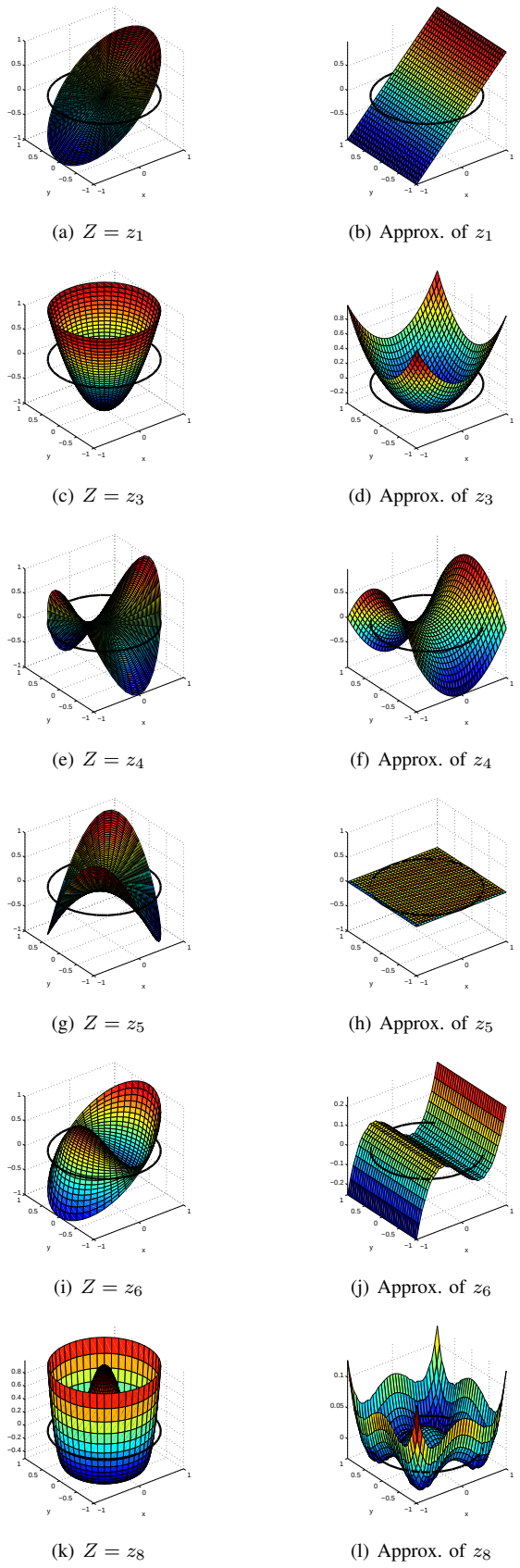

(a) $Z = z_1$ (b) Approx. of z_1

(c) $Z = z_3$ (d) Approx. of z_3

(e) $Z = z_4$ (f) Approx. of z_4

(g) $Z = z_5$ (h) Approx. of z_5

(i) $Z = z_6$ (j) Approx. of z_6

(k) $Z = z_8$ (l) Approx. of z_8

Fig. 3. Examples of OPA Zernike approximations. The Pure Zernikes are on the left and their OPA approximations are on the right. The error corresponding to each approximation is: (b) 2.5×10^{-10}, (d) 1.3×10^{-10}, (f) 1.9×10^{-10}, (h) 33.1, (j) 3.1, (l) 0.62

$$H(s) = \frac{K(\frac{1}{\tau})}{s + (\frac{1}{\tau})} \tag{13}$$

$$\tau = \begin{cases} \tau_{rise} & \text{if} \quad crystal \Uparrow \\ \tau_{fall} & \text{if} \quad crystal \Downarrow \end{cases} \tag{14}$$

B. Simulation

In simulation, a source of aberrations had to be developed. This was accomplished by randomly selecting the Zernike coefficients a_i for the first sixteen Zernikes described in Table I. The resulting aberration from (1) was then scaled to limit the peaks of the aberration between $-\pi$ and π. Here the assumption is made that aberrations in the system will not exceed these bounds. This random abberation is then used to create an aberrated image with (2), (3), and (4). Now the randomly generated phase profile created for aberration can be considered to be unknown and the simulation begins assuming the object is known and the aberrated image has been received at a camera. Next the phase profile is reconstructed with (5). It is then fit to the first 11 Zernike coefficients, which is then fit to an OPA Zernike representation. The negative representation is written to the OPA and the wavefront is corrected as the crystals settle into the commanded position.

C. Results

Fig. 4 is a summary of results from a simulation of the wavefront correction algorithm. The original point-source objects with intensity levels of 1.0 are shown in contour and surface views in Figs. 4(a) and 4(b). After being exposed to an aberration, the the resulting image in Figs. 4(c) and 4(d) experiences a power drop to 0.28 with an error of 12.5. After phase reconstruction, a depiction of the aberration profile is available in Fig. 4(e). There is a complete loss of the lump-like feature in the center of the phase plane when the recovered phase profile is fitted with only the first eleven Zernike coefficients, Fig. 4(f). The OPA command to correct the aberration is shown in Fig. 4(g). Note that the OPA representation loses the bowl-like feature of the recovered phase profile. That combined with the loss of the lump-like feature are the source of some imperfections in the corrected image in Figs. 4(h) and 4(i). Despite the losses due to the OPA limitations, the intensity of the image is restored to 0.51 and the error is reduced to 6.5.

Considering the system dynamics and the difficulty the OPA had in depicting the desired phase profile, the algorithm took about 20 milliseconds to converge. In Fig. 5, the intensity and the error converge to the final values in an exponential manner. Notice the slight decrease in intensity in the first few iterations of the simulation. This is due to the reorientation of the crystals and is not a source for concern as the error of the corrected image is constantly decreasing.

In another simulation shown in Fig. 6, the random aberration is changed every 20 milliseconds and the algorithm is left to correct for each new aberration. It is interesting to note that despite the differences in "rising" and "falling" liquid crystal dynamics, there is no obvious

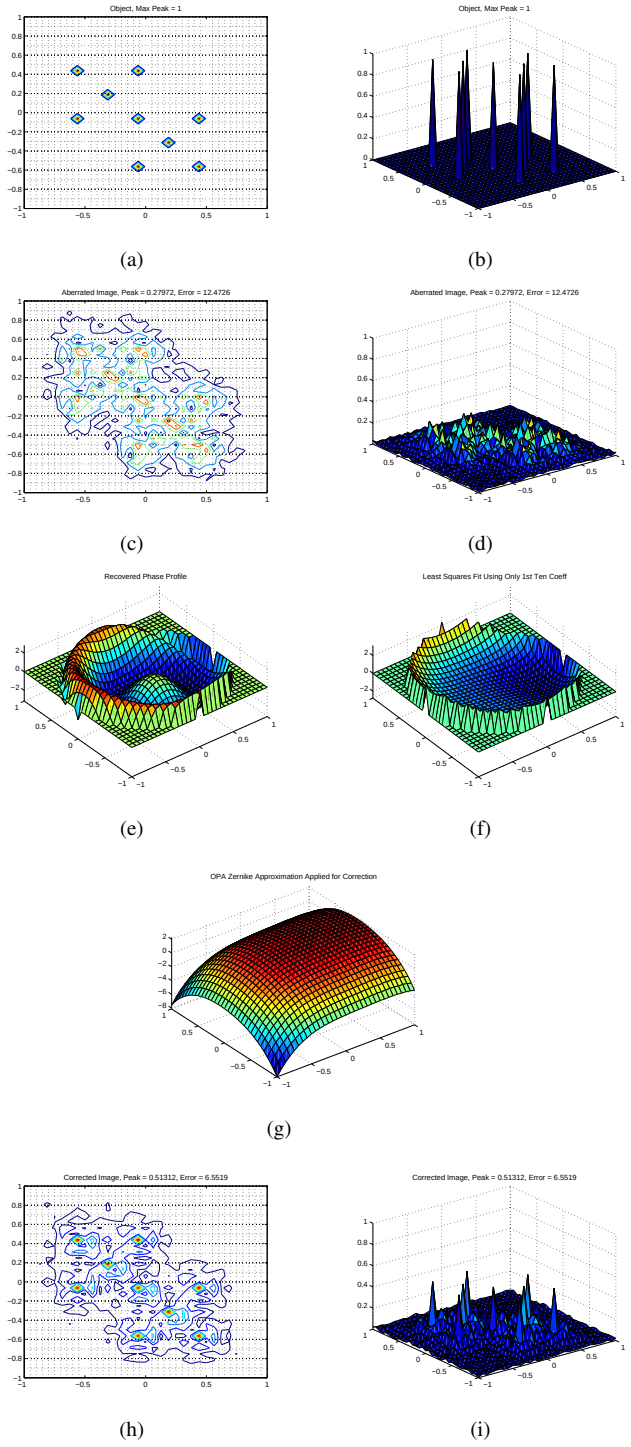

Fig. 4. Simulation results: (a) & (b): The original object with intensity 1.0 shown as a contour and surface plot. (c) & (d): The aberrated image with intensity 0.28 and an error of 12.5. (e): The recovered phase profile associated with the aberration. (f): The least squares fit to the first eleven Zernikes, note the loss of the of the lump-like feature in the center of the plane. (g): The negative OPA representation of (f) which is written to the OPA as a command. (h) & (i): The corrected image with intensity 0.51 and an error of 6.5.

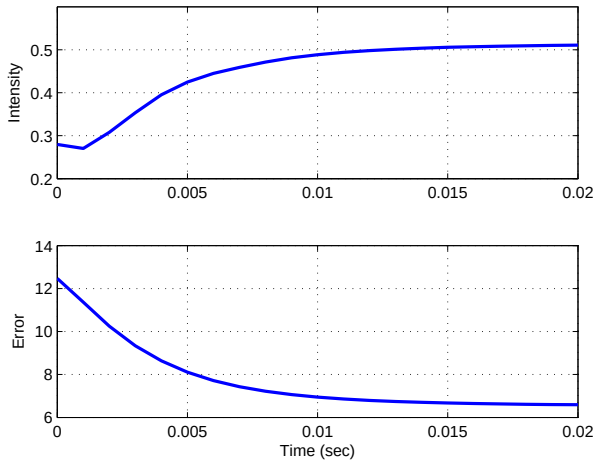

Fig. 5. Simulation results: The dynamics of the liquid crystals are evident here. The intensity can be seen converging to the final value in 20 milliseconds (top) while the error of the correction continually drops (bottom).

change in the settle time of the correction. The differences in converging values for intensity and error in Fig. 6 is a reminder that the success of this technique is heavily dependent on the OPA's ability to represent the aberration in the system.

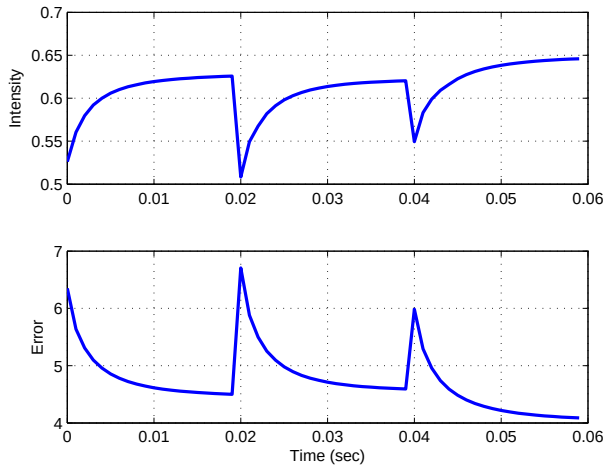

Fig. 6. Simulation results: The random aberration is varied every 20 milliseconds and the algorithm works to correct for the changes. Note that despite the differences in "rising" and "falling" liquid crystal dynamics the settle times for the intensity (top) and the (error) are essentially the same.

VII. Conclusions and Future Work

A. Conclusions

Simulations show that the proposed technique for wavefront aberration correction of point sources performs well and shows improvement of the wavefront in all situations. However, it is clear that the effectiveness of the technique is severely restricted by the limitations of the OPA. Specifically, the dependent pixel relationship of the OPAs is the major source of the occasional limited success of the algorithm. If the OPA had the ability to perfectly represent the first eleven Zernike polynomials, the proposed method would perform almost without flaw. However, as Fig. 3 indicates the beamsteering device struggles to represent many of the first eleven Zernikes, and performance declines. Perhaps the use of three OPAs mounted in an offset of 60 degrees from each other or a pixelated spatial light modulator as used in previous work by Love [6] would offer more success.

B. Future Work

The next step is to preform system identification on the Boulder Nonlinear Systems OPA to obtain a better model of the liquid crystal dynamics. As the crystals are currently modelled, much of the interesting dynamics are lost. The model used in the simulations is sufficient for a proof of concept, but the actual dynamics of the OPA must eventually be addressed. In addition, once an more accurate model of the crystal dynamics exists, work can begin on developing an elegant controller which will speed the response to aberrations in the system. Ideally, the settling time in Fig. 5 can be vastly improved, and validated experimentally.

References

[1] P. McManamon, T. Dorshner, *et al.*, "Optical Phased Array Technology", *Proc. IEEE*, vol. 84, no. 2, 1996, pp 268-298.

[2] Boulder Nonlinear Systems, 450 Courtney Way Unit #107, Lafayette, CO 80026, http://www.bnonlinear.com/

[3] B. Wandernoth, and P. Oleski, "Performance Evaluation of a Liquid Crystal Beam Steering/Beam Spoiling Device Developed for Space Communication Applications", *Proc. SPIE*, vol. 2699, 1996, pp 240-257.

[4] R. Shannon, J. Wyant, *Applied Optics and Optical Engineering, Vol. XI*, Academic Press, 1992.

[5] S. Harris, "Characterizing and Application of a Liquid Crystal Beam Steering Device", *Proc. SPIE*, vol. 4291, 2001, pp 109-119.

[6] G. Love, "Wave-front Correction and Production of Zernike Modes with a Liquid-Crystal Spatial Light Modulator", *Applied Optics*, vol. 36, no. 7, 1997, pp 1517-1524.